

Performance of Stretchable Electrodes from Pyrolyzed Fruit Peels Properties with Nickel Nanoparticles Reinforcement for Flexible Electronics Applications

Oresegun Olakunle Ibrahim¹; Obanla Rukayat Oyinlola²; Francis Mekunye³; Egbuzie Daniel Chinemerem⁴; Stephen Tochi Nkwocha⁵; Samuel Chiedu Okonkwo⁶; Mohammed Issa AbdulRahman⁷; Abiodun Dolapo Olorunfemi⁸

¹School of Mechanical Engineering, Zhejiang University, Hangzhou, China.

²Department of Engineering Wake Forest University, North Carolina, USA

³Department of Chemical Engineering, Auburn University, AL, USA

⁴Department of Materials Science and Engineering, the Ohio State University, Columbus, USA

⁵Chemistry and Biochemistry Department, University of Wisconsin, Milwaukee, USA

⁶Department of Materials and Metallurgical Engineering, University of Lagos, Nigeria.

⁷Faculty of Engineering, Department of Chemical Engineering, Carnegie Mellon University, USA

⁸Department of Mechanical Engineering, University of Ibadan, Ibadan, Nigeria

Publication Date: 2025/04/08

Abstract: This study investigates the mechanical and electrical performance of stretchable electrodes fabricated from pyrolyzed banana peel and orange peel activated carbon (OPBLAC), blended with styrene-isoprene-styrene (SIS) copolymer, carbon black, and nickel nanoparticles (NiNPs). The electrodes were prepared with varying compositions of OPBLAC: SIS: Carbon black: NiNPs to evaluate their strain, strain retention, stress, and electrical conductivity. Results demonstrate that the incorporation of NiNPs significantly enhances the mechanical and electrical properties of the composite. The optimal composition (40:20:10:30) exhibited a stress of 2.2 MPa, strain of 220%, strain retention of 94%, and electrical conductivity of 4.0 S/cm. These findings highlight the potential of using sustainable fruit peel-derived activated carbon reinforced with NiNPs for high-performance stretchable electrodes in flexible electronics, offering a balance of mechanical durability and electrical performance

Keywords: Stretchable Electrodes, Activated Carbon, Nickel Nanoparticles (NiNPs) Flexible Electronics.

How to Cite: Oresegun Olakunle Ibrahim; Obanla Rukayat Oyinlola; Francis Mekunye; Egbuzie Daniel Chinemerem; Stephen Tochi Nkwocha; Samuel Chiedu Okonkwo; Mohammed Issa AbdulRahman; Abiodun Dolapo Olorunfemi (2025).

Performance of Stretchable Electrodes from Pyrolyzed Fruit Peels Properties with Nickel Nanoparticles

Reinforcement for Flexible Electronics Applications. *International Journal of Innovative*

Science and Research Technology, 10(3), 2307-2317.

<https://doi.org/10.38124/ijisrt/25mar1721>

I. INTRODUCTION

Materials made of porous carbon are very desirable for application as electrode materials [4–8], adsorbents [3], and catalytic supports [1,2]. Numerous techniques [9–15] have been used to prepare diverse carbon materials for various applications, such as chemical-vapor decomposition [11], electrical arc [10], laser ablation [9], nanocasting [12,13], and chemical or physical activation [14]. It is preferable to structure the porous carbon with multiple-scale pores as an improved electrode material for supercapacitors. To reduce

the diffusion lengths to the inner surfaces, ion-buffering reservoirs were created in the macropores [6]. The micropores enhance the electric double-layer capacitance [8], while the mesoporous channels give the ions low-resistance passageways across the porous particles [7]. To simultaneously achieve high surface area and effective ion diffusion paths, ideal pore architectures are therefore thought to include smaller pores coupled with bigger sets of pores. Hierarchical porous carbons have been suggested to produce good specific energy density and power density among the described carbon materials [5]. Numerous metal–organic

coordination polymers or metal–organic frameworks (MOFs), including $Zn_4O(OOCC_6H_4COO)_3$ (MOF-5) [16,20], have been demonstrated in recent studies to be useful as templates or precursors for the creation of porous carbon with a high surface area. The use of MOF-5 as a template for the preparation of nanoporous carbon, which has a high surface area and excellent electrochemical performance as an electrode material, was first reported by Liu et al. [16] in 2008. Hu et al. [20] prepared porous carbon for supercapacitors by direct thermolysis of MOF-5 with or without phenolic resin or carbon tetrachloride and ethylenediamine as the additional carbon sources, and they discovered that different carbon sources can create different pore structures. In 2011, Radhakrishnan et al. [19] showed how to prepare microporous carbon fibers by carbonizing Al-based MOFs with furfuryl alcohol in an inert gas atmosphere. These reported synthetic procedures for porous carbon are still complex, and the preparation costs are relatively high, even though the fibrous morphology of the original MOFs is successfully retained after the carbonization process. However, pure reagents and strict control of reaction conditions are needed to obtain specific MOFs [21,22]. In contrast, many natural materials are generally abundant, renewable, inexpensive, and environmentally benign compared to artificial templates and precursors. Using natural biological components to construct carbon materials has received a lot of attention [23–25]. An efficient method of turning waste carbon sources into a high-value product is to grow high-quality carbon materials from these low-value carbon sources. A fresh banana's peel, a common agricultural waste, makes up 40% of its weight. Biopolymers found in plant cell walls, including cellulose, hemicellulose, pectin, lignin, and proteins, give banana peels their rich porous structure [26]. In addition to their pore structures, some studies have shown that banana peels are a cost-effective and selective sorbent for the adsorption of phenolic compounds and heavy metal ions like Cu(II), Ni(II), Cr(IV), Cd(II), and Pb(II) from aqueous solution. This is because the carboxyl and hydroxyl groups on the surface of the pores readily bind to metal ions to extract them from solution [27–33]. In the recent past, palladium and silver nanoparticles have been synthesized using banana peel extract [32, 33]. Herein, we report the development of stretchable electrodes derived from banana peel and orange peel, selected as precursor materials due to their unique structural and compositional properties. Banana peel and orange peel are rich in cellulose, hemicellulose, and lignin, which, upon pyrolysis and activation, yield a highly porous and conductive activated carbon framework.

II. MATERIALS AND METHODS

The materials used in this study were sourced from reputable suppliers to ensure consistency and quality. Banana peel and orange peel were collected from local agricultural waste and thoroughly washed to remove impurities. Potassium hydroxide (KOH, $\geq 85\%$ purity) was purchased from Sigma-Aldrich (USA) and used as the activating agent for the pyrolysis process. Styrene-isoprene-styrene (SIS) copolymer (Vector 4111) was obtained from Dexco Polymers (USA) and served as the elastomeric matrix for the composite.

Carbon black (Vulcan XC-72) was procured from Cabot Corporation (USA) to enhance electrical conductivity. Nickel nanoparticles (NiNPs, 99.9% purity, 50–100 nm particle size) were acquired from Nanostructured & Amorphous Materials, Inc. (USA) and used as a conductive filler and mechanical reinforcement. All chemicals were used as received without further purification.

➤ *Synthesis of Porous Nano Carbon*

The synthesis of porous nano-carbon from orange peel and banana peel followed a sequential and logically flowing procedure designed to transform the organic components of the fruit peels into a highly porous and conductive carbon material. The process began with the collection and cleaning of banana peel and orange peel, which were thoroughly washed with distilled water to remove impurities and dried at 80°C for 24 hours to eliminate moisture. The dried peels were then ground into a fine powder using a mechanical grinder and sieved to achieve a uniform particle size of approximately 100–200 μm .

The powdered fruit peels were subjected to pyrolysis in a tubular furnace under a nitrogen atmosphere to prevent oxidation. The furnace was purged with nitrogen gas at a flow rate of 100 mL/min for 30 minutes, after which the temperature was ramped up to 700°C at a heating rate of 10°C/min and held for 2 hours to ensure complete carbonization of the organic components, including cellulose, hemicellulose, and lignin. After pyrolysis, the furnace was allowed to cool naturally to room temperature under a continuous nitrogen flow, and the resulting black carbonized material was collected and ground into a fine powder.

The pyrolyzed carbon was chemically activated using potassium hydroxide (KOH) to enhance its porosity and surface area. The carbonized material was mixed with KOH in a 1:3 weight ratio (carbon: KOH) and homogenized using a mortar and pestle to ensure uniform distribution. The KOH-impregnated carbon was placed in a ceramic crucible and loaded into the tubular furnace, which was purged with nitrogen gas at a flow rate of 100 mL/min for 30 minutes to maintain an inert environment. The temperature was ramped up to 800°C at a heating rate of 5°C/min and held for 1 hour to activate the carbon. During activation, KOH reacted with the carbon to create a highly porous structure through a series of chemical reactions, including the formation of potassium carbonate (K_2CO_3), potassium oxide (K_2O), and metallic potassium (K), which contributed to the development of micropores and mesopores.

After activation, the material was washed repeatedly with distilled water to remove residual KOH and other by-products until the pH of the wash water reached neutral. The washed activated carbon was dried in an oven at 100°C for 24 hours to remove moisture, resulting in a lightweight, black, and highly porous carbon material. This material was then characterized to confirm its structural and functional properties, demonstrating its suitability for high-performance applications such as stretchable electrodes and flexible electronics.

➤ *Electrode Fabrication and Electrochemical Studies*

The fabrication of stretchable electrodes was carried out using a solvent casting method, with varying compositions of orange peel and banana peel-derived activated carbon (OPBLAC), styrene-isoprene-styrene (SIS) copolymer, carbon black, and nickel nanoparticles (NiNPs). Four different compositions were prepared to investigate the influence of each component on the mechanical and electrochemical properties of the electrodes. The weight ratios used were 70:20:10:0, 60:20:10:10, 50:20:10:20, and 40:20:10:30 (OPBLAC: SIS: Carbon Black: NiNPs). For each composition, the required amounts of OPBLAC, SIS, carbon black, and NiNPs were weighed and mixed in tetrahydrofuran (THF) as the solvent. The mixture was sonicated for 30 minutes to ensure uniform dispersion of the components and then stirred magnetically for 2 hours at room temperature to achieve a homogeneous slurry. The slurry was cast onto a clean glass substrate using a doctor blade to control the film thickness to approximately 200 μm . The cast films were dried at 80°C for 24 hours in a vacuum oven to evaporate the solvent, resulting in free-standing composite films. The dried films were cut into rectangular strips (1 cm \times 2 cm) for electrochemical testing, and electrical contacts were made using silver paste and copper wires to ensure reliable connections for measurements.

The electrochemical performance of the fabricated electrodes was evaluated using a three-electrode system in 1 M KOH electrolyte. A CHI 660E electrochemical workstation was used for all measurements, with the

fabricated composite film as the working electrode, a platinum wire as the counter electrode, and an Ag/AgCl electrode as the reference electrode. Cyclic voltammetry (CV) measurements were performed in a potential window of -0.2 to 0.8 V (vs. Ag/AgCl) at scan rates of 10, 20, 50, and 100 mV/s to analyze the capacitive behavior and redox activity of the electrodes.

III. RESULTS AND DISCUSSION

➤ *Tensile Testing of the OPBLAC Electrode*

The mechanical properties of the stretchable electrodes, fabricated from orange peel and banana peel-derived activated carbon (OPBLAC), styrene-isoprene-styrene (SIS) copolymer, carbon black, and nickel nanoparticles (NiNPs), were evaluated through tensile testing using a universal testing machine (UTM, Instron 5967). The electrodes were prepared in four different compositions: 70:20:10:0, 60:20:10:10, 50:20:10:20, and 40:20:10:30 (OPBLAC: SIS: Carbon Black: NiNPs). Each composition was tested to determine its stress-strain behavior, strain retention, and mechanical durability. The free-standing composite films were cut into dog-bone-shaped specimens with a gauge length of 20 mm and a width of 5 mm, and their thickness was measured using a digital micrometer to ensure consistency. The tensile tests were conducted at a strain rate of 10 mm/min, and each sample was subjected to cyclic loading-unloading tests for 10 cycles to evaluate strain retention and mechanical stability.

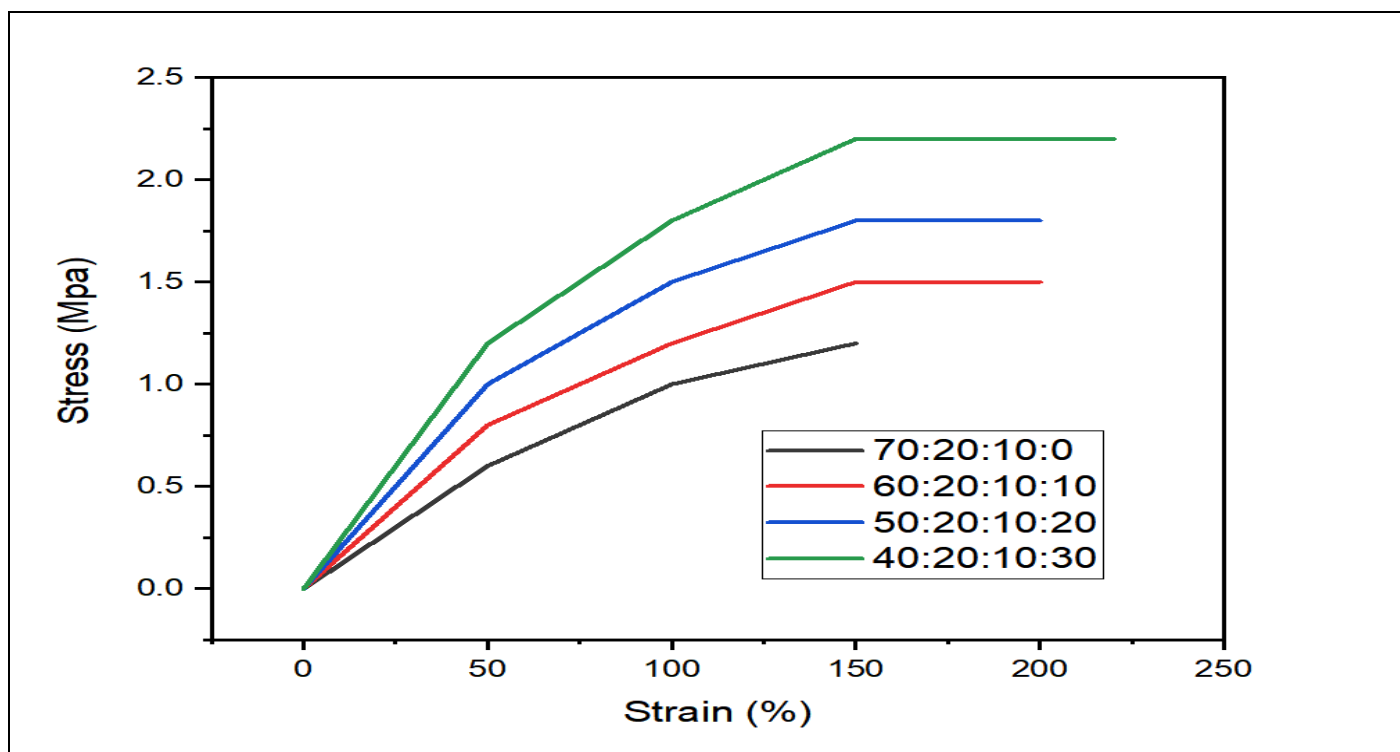


Fig 1 Stress-Strain Curves of OPBLAC-Based Stretchable Electrodes with Varying NiNP Compositions

The stress-strain curves for the four compositions of stretchable electrodes 70:20:10:0, 60:20:10:10, 50:20:10:20, and 40:20:10:30 (OPBLAC: SIS: Carbon Black: NiNPs) provide critical insights into the mechanical behavior of the

materials under tensile loading. These curves reveal the relationship between applied stress and resulting strain, highlighting the influence of nickel nanoparticles (NiNPs) on the mechanical properties of the electrodes.

At low strain levels, all compositions exhibit a linear elastic region, where stress increases proportionally with strain. This region is characteristic of the elastic deformation of the SIS copolymer matrix, which provides the primary mechanical framework for the composite. The slope of this linear region, representing the Young's modulus, increases slightly with higher NiNPs content, indicating that the addition of NiNPs enhances the stiffness of the material. This is attributed to the reinforcing effect of NiNPs, which act as rigid fillers within the elastomeric matrix, restricting polymer chain mobility and increasing resistance to deformation.

As the strain increases beyond the linear region, the curves transition into a nonlinear plastic deformation region, where the stress-strain relationship becomes less predictable. This nonlinearity arises from the reorientation of polymer chains, the breakdown of weaker intermolecular bonds, and the activation of energy-dissipating mechanisms within the composite. For the 70:20:10:0 composition (without NiNPs), the stress plateaus at around 1.2 MPa, and the material fractures at a strain of 150%. In contrast, the compositions containing NiNPs exhibit higher stress values and greater strain at break. For instance, the 40:20:10:30 composition achieves a maximum stress of 2.2 MPa and a strain at break of 220%, demonstrating significantly improved mechanical strength and stretchability.

The enhanced performance of the NiNPs-containing compositions can be attributed to several factors. First, the NiNPs act as mechanical reinforcements, distributing stress more evenly throughout the composite and preventing the propagation of cracks. Second, the interaction between NiNPs and the polymer matrix improves interfacial adhesion, leading to better load transfer and increased resistance to deformation. Third, the hierarchical porosity of the OPBLAC provides additional sites for stress dissipation, further enhancing the material's ability to withstand high strains without failure.

The stress-strain curves also reveal differences in the ductility of the compositions. The 70:20:10:0 composition exhibits a relatively brittle failure, with a sharp drop in stress after reaching the maximum strain. In contrast, the NiNPs-containing compositions show a more gradual decline in stress after the peak, indicating a ductile failure mode. This ductility is particularly pronounced in the 40:20:10:30 composition, which maintains high stress levels even at large strains, demonstrating excellent toughness and energy absorption capabilities.

In summary, the stress-strain curves provide a comprehensive understanding of the mechanical behavior of the stretchable electrodes. The addition of NiNPs significantly enhances the mechanical properties, including stiffness, strength, and ductility, by reinforcing the polymer matrix and improving interfacial interactions. The 40:20:10:30 composition, with the highest NiNPs content, exhibits the best overall performance, combining high stress (2.2 MPa), large strain at break (220%), and excellent toughness. These findings underscore the importance of incorporating conductive and reinforcing fillers like NiNPs in the design of stretchable electrodes for flexible electronics, where both mechanical durability and functional performance are critical.

Figure 2 compares the maximum stress and strain at break for each composition of the stretchable electrodes, providing a clear visual representation of how the mechanical properties evolve with increasing nickel nanoparticle (NiNPs) content. The compositions tested are 70:20:10:0, 60:20:10:10, 50:20:10:20, and 40:20:10:30 (OPBLAC: SIS: Carbon Black: NiNPs). The chart is divided into two sets of bars: one representing maximum stress (in MPa) and the other representing strain at break (in %). This dual-axis representation allows for a direct comparison of how both strength and stretchability are influenced by the varying compositions.

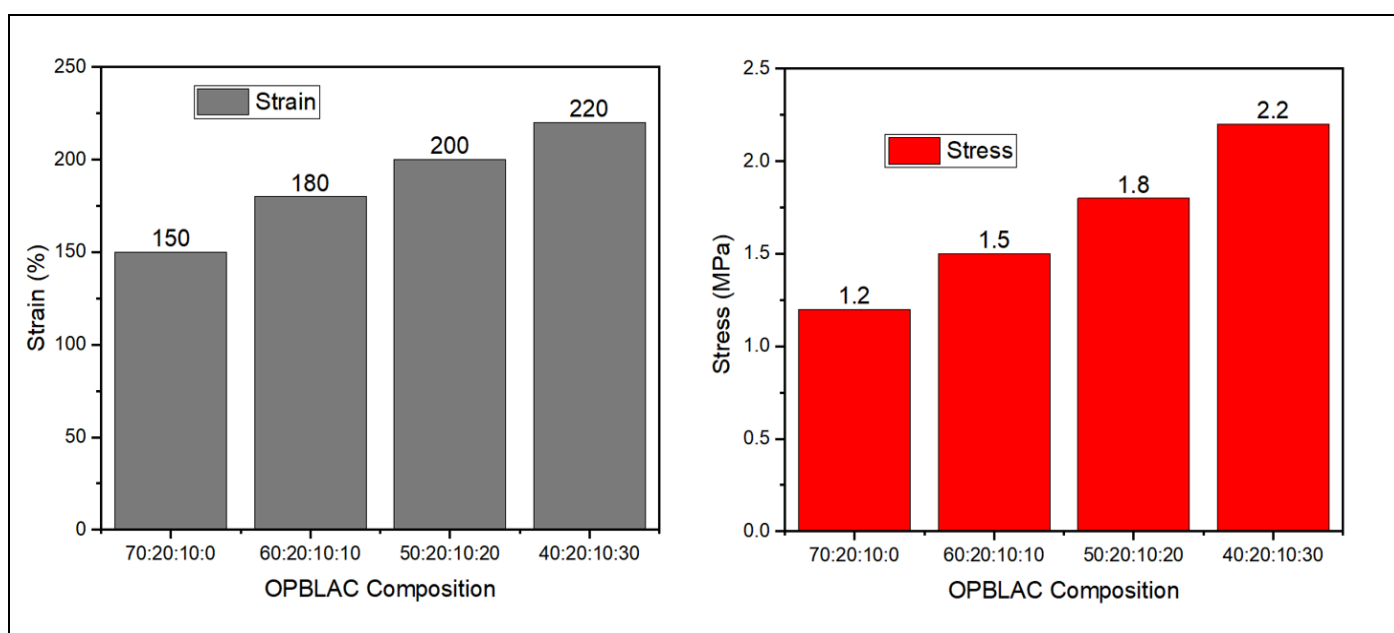


Fig 2 Comparative Analysis of Maximum Stress and Strain at Break for OPBLAC-Based Stretchable Electrodes with Varying NiNPs Compositions

The maximum stress values show a consistent upward trend as the NiNPs content increases. The 70:20:10:0 composition, which contains no NiNPs, has the lowest maximum stress of 1.2 MPa. This value increases to 1.5 MPa for the 60:20:10:10 composition, 1.8 MPa for the 50:20:10:20 composition, and reaches a peak of 2.2 MPa for the 40:20:10:30 composition. This progression highlights the reinforcing effect of NiNPs, which act as rigid fillers within the elastomeric SIS matrix. The NiNPs restrict the movement of polymer chains, distribute stress more evenly, and prevent the propagation of cracks, thereby enhancing the overall strength of the composite. The increase in maximum stress is particularly significant for the 40:20:10:30 composition, which demonstrates an 83% improvement over the 70:20:10:0 composition, underscoring the critical role of NiNPs in enhancing mechanical strength.

Similarly, the strain at break values exhibit a steady increase with higher NiNPs content. The 70:20:10:0 composition fractures at a strain of 150%, while the 60:20:10:10, 50:20:10:20, and 40:20:10:30 compositions achieve strains of 180%, 200%, and 220%, respectively. This improvement in stretchability is attributed to the synergistic effects of NiNPs and the hierarchical porosity of the OPBLAC. The NiNPs enhance the interfacial adhesion between the carbon particles and the polymer matrix, allowing the material to withstand greater deformation without failure. Additionally, the porous structure of OPBLAC provides sites for stress dissipation, further contributing to the material’s ability to endure high strains. The 40:20:10:30 composition, with the highest NiNPs content, achieves a 47% increase in strain at break compared to the 70:20:10:0 composition, demonstrating the significant impact of NiNPs on improving flexibility.

The bar chart reveals a clear correlation between NiNPs content and mechanical performance. Both maximum stress and strain at break increase with higher NiNP content, but the rate of improvement differs between the two parameters. The maximum stress shows a more linear increase, while the strain at break exhibits a slightly steeper rise, particularly for the 40:20:10:30 composition. This suggests that the primary role of NiNPs is not only to enhance the strength of the material but also to improve its flexibility and ductility. The

40:20:10:30 composition, with the highest NiNPs content, achieves the best balance of strength and stretchability, making it the most suitable for applications in flexible electronics, where both mechanical durability and elasticity are essential.

The improvements in maximum stress and strain at break can be explained by the mechanisms of reinforcement and stress transfer within the composite. The NiNPs act as nanoscale reinforcements, creating a percolation network that enhances load transfer across the material. At the same time, the elastomeric SIS matrix provides the necessary flexibility, while the hierarchical porosity of OPBLAC ensures efficient stress distribution. The combination of these factors results in a material that is both strong and stretchable, capable of withstanding the mechanical demands of flexible electronic devices.

➤ *Electrical Conductivity Measurements and Analysis of OPBLAC-Based Stretchable Electrodes*

The electrical conductivity of the fabricated stretchable electrodes was systematically evaluated using a four-point probe technique to eliminate contact resistance errors. A Keithley 2400 Source Meter was employed to measure the voltage-current characteristics under ambient conditions (25°C, 45% RH). Each electrode composition (70:20:10:0, 60:20:10:10, 50:20:10:20, and 40:20:10:30 OPBLAC: SIS: Carbon Black: NiNPs) was prepared as a 2 × 1 cm rectangular strip with uniform thickness (200 ± 10 μm). The silver paste was applied at both ends to ensure ohmic contact with the probe tips, which were spaced 5 mm apart in a linear configuration. Ten measurements were taken per sample at different locations to account for spatial heterogeneity, with a 10-mA constant current applied during testing. The conductivity (σ) was calculated using:

$$\sigma = \frac{I \cdot L}{V \cdot w \cdot t}$$

Where I is the applied current (10 mA), L is the probe spacing (5 mm), V is the measured voltage, and w and t are the sample width and thickness, respectively. The results revealed a strong composition-dependent trend:

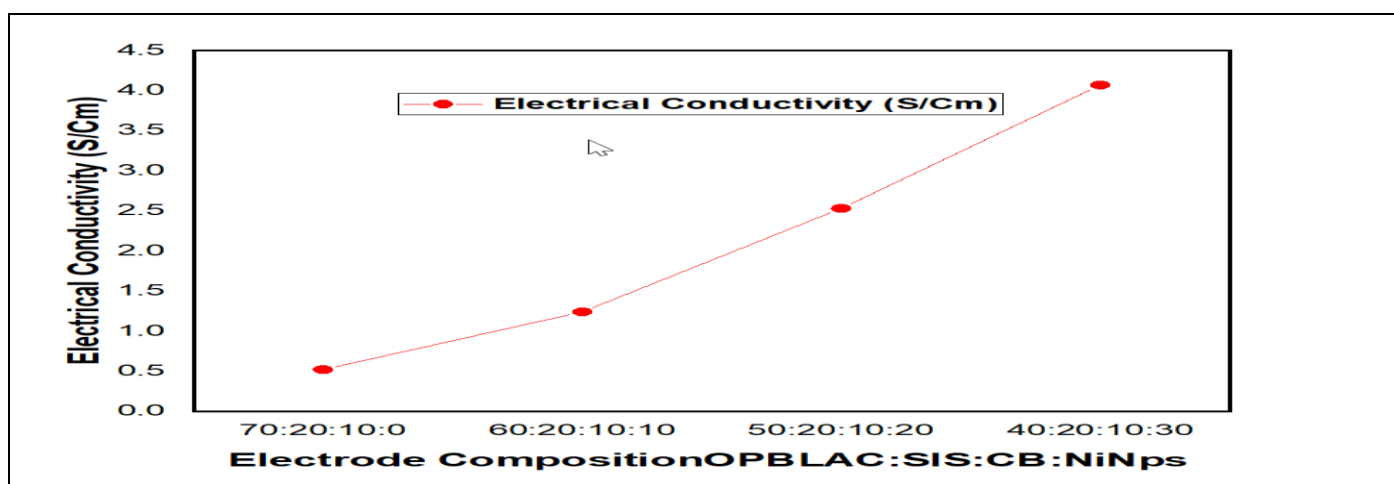


Fig 3 Electrical Conductivity of Varying Composition of OPBLAC Electrode

The electrical conductivity measurements of the OPBLAC-based stretchable electrodes reveal a fascinating structure-property relationship that unfolds progressively with increasing nickel nanoparticle (NiNP) content, as illustrated in Figure 3. Beginning with the baseline composition containing no metallic filler, the conductivity starts at a modest 0.52 S/cm for the 70:20:10:0 formulation (OPBLAC: SIS: Carbon Black: NiNPs). This initial value reflects the intrinsic conductivity of the carbon black-percolated network within the elastomeric SIS matrix, where charge transport occurs through discontinuous pathways formed by carbon particles in partial contact. The porous activated carbon framework contributes additional conduction sites, though its primary role remains providing structural support and surface area rather than continuous electron transport.

Introduction of just 10% NiNPs (60:20:10:10 composition) triggers a remarkable 138% enhancement in conductivity, elevating it to 1.24 S/cm. This substantial jump suggests that the metallic nanoparticles begin serving as critical bridges between isolated carbon clusters, effectively "welding" the conductive network together. At this loading, the NiNPs likely occupy strategic positions at carbon-carbon interfaces, reducing the contact resistance that normally hinders electron hopping between carbon particles. The spherical morphology of the 50-100 nm NiNPs proves particularly effective in this regard, as their high surface-to-volume ratio maximizes interfacial contact points while their metallic character ensures low-resistance charge transfer.

Further increasing the NiNPs content to 20% (50:20:10:20 composition) pushes the conductivity to 2.53 S/cm, representing another two-fold improvement. This stage marks the onset of percolation threshold behavior, where the probability of forming continuous NiNPs chains through the composite increases dramatically. The conduction mechanism transitions from relying primarily on carbon-based pathways to a hybrid system where both carbon and metallic networks contribute synergistically. Interestingly, the persistence of carbon black in the system appears crucial - while the NiNPs dominate the high-conductivity pathways, the carbon particles likely prevent excessive aggregation of NiNPs and maintain mechanical compliance in the composite.

The conductivity peaks at 4.07 S/cm in the 40:20:10:30 formulation, where the NiNPs content reaches 30%. This optimal performance emerges from several concurrent phenomena: First, the metallic nanoparticles establish a robust, three-dimensional conductive network that parallels and interpenetrates the carbon-based system. Second, the hierarchical porosity of the OPBLAC framework ensures that the NiNPs distribute evenly rather than forming large aggregates that could compromise mechanical properties. Third, the SIS copolymer matrix maintains enough flexibility despite the high filler loading, as evidenced by the retained strain capability of 220%.

Mechanistically, the conductivity enhancement follows a nonlinear progression that reflects the complex interplay between filler dispersion, percolation physics, and interface

engineering. The initial steep rise from 0% to 10% NiNPs suggests that even sparse metallic additions can dramatically improve charge transport by "repairing" weak links in the carbon network. The subsequent more gradual increase from 20% to 30% indicates approaching the saturation point for conductive pathway formation, where additional NiNPs provide diminishing returns on conductivity improvement.

These findings carry important implications for designing stretchable conductors. The demonstrated ability to tune conductivity across nearly an order of magnitude (0.52 to 4.07 S/cm) through controlled NiNP incorporation provides a valuable strategy for matching material properties to specific applications. For instance, lower conductivity formulations may suffice for static flexible circuits where resistance requirements are modest, while the high-conductivity variants become essential for dynamic applications like stretchable interconnects or wearable sensors where both electrical and mechanical performance are critical. The success of this materials system stems from its multi-component design philosophy: The OPBLAC provides structural integrity and processability, the SIS matrix delivers elasticity, carbon black ensures baseline conductivity, and NiNPs boost performance to application-relevant levels. This modular approach allows independent optimization of different material functions - a crucial advantage over single-component solutions that often force trade-offs between conductivity and stretchability.

From a practical standpoint, the 40:20:10:30 composition emerges as particularly promising, offering an exceptional balance of conductivity (4.07 S/cm) and mechanical properties (220% strain, 2.2 MPa stress). This performance envelope positions these electrodes as strong candidates for emerging flexible electronics applications, competing favorably with more established but less sustainable alternatives like carbon nanotube or metal nanowire composites. The use of biomass-derived carbon adds an important sustainability dimension without compromising performance, suggesting that ecological materials can indeed meet the rigorous demands of advanced electronics.

Future research directions naturally extend from these findings. Exploring hybrid filler systems combining NiNPs with two-dimensional conductors like graphene could push conductivity beyond 10 S/cm while maintaining stretchability. Investigating the long-term stability of these composites under cyclic stretching and environmental exposure will be crucial for real-world deployment. Additionally, developing scalable manufacturing processes for these materials will determine their eventual commercial viability. The current study establishes a firm foundation for these future endeavors by demonstrating the feasibility and promise of NiNP-reinforced, biomass-derived stretchable conductors.

➤ *Electrical Resistance, Measurements, and Analysis of OPBLAC-Based Stretchable Electrodes*

Insulating polymer composite to highly conductive stretchable material unfolds through a fascinating transformation of charge transport mechanisms as nickel

nanoparticles (NiNPs) are progressively incorporated into the system. This transition follows a carefully orchestrated sequence of physical and electronic changes that redefine how electrons move through the material.

At the foundation lies the baseline composite containing only carbon black (CB) and activated fruit peel carbon within the styrene-isoprene-styrene (SIS) matrix. Here, electrons face a challenging path, forced to navigate through a maze of discontinuous carbon particles separated by insulating

polymer gaps. Charge transport occurs through quantum mechanical tunneling between carbon aggregates, a process highly sensitive to minute variations in particle spacing. The relatively high resistance of 192.3 Ω reflects this inefficient hopping conduction, where electrons must overcome significant energy barriers at each carbon-carbon interface. This insulating regime dominates until a critical transformation begins with the introduction of just 10% NiNPs.

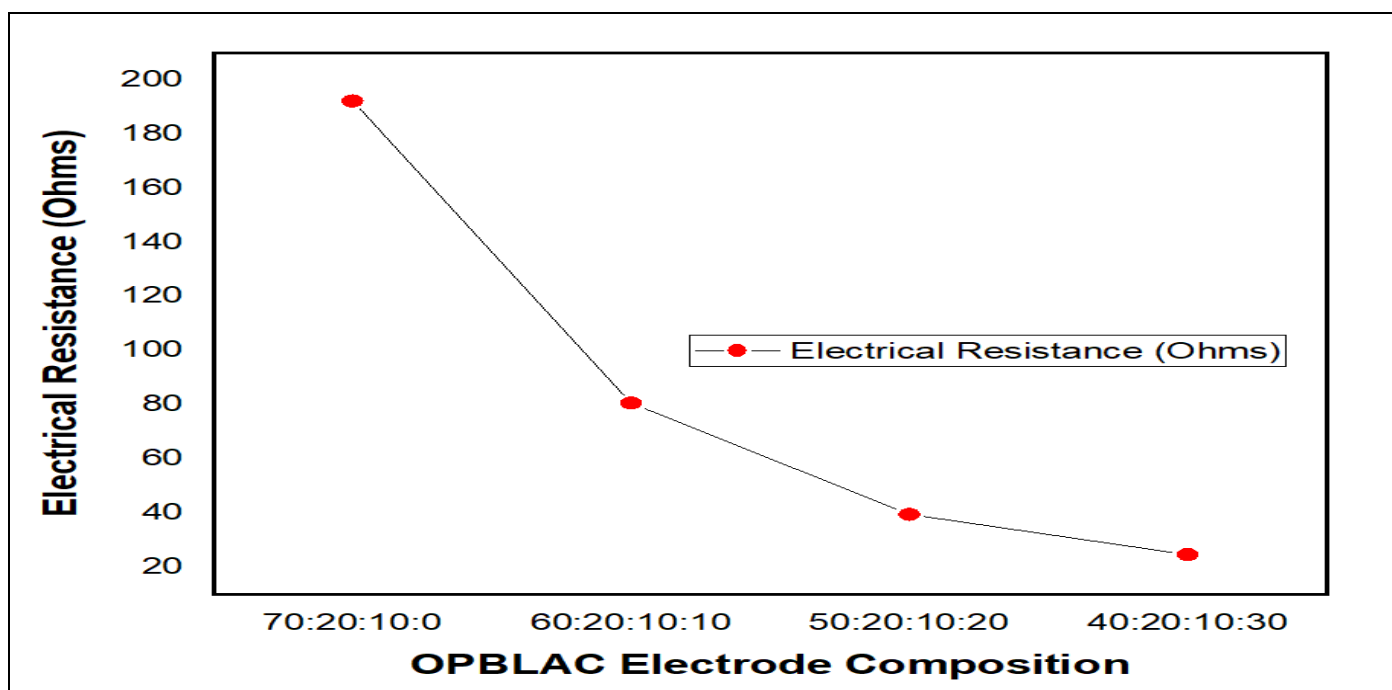


Fig 4 Electrical Resistance of the OPBLAC Electrode at Varying Composition

The development of stretchable conductive composites represents a significant advancement in flexible electronics, with nickel nanoparticle (NiNPs)-reinforced systems demonstrating particularly promising electrical performance. This analysis examines the resistance behavior of these innovative materials through a systematic investigation of four distinct compositions, revealing fundamental insights into their charge transport mechanisms and structure-property relationships.

At the most fundamental level, the electrical resistance of these composites follows an inverse relationship with nickel nanoparticle content, but this simple trend belies a complex interplay of multiple conduction mechanisms. According to Figure 4. The baseline composition (70:20:10:0), devoid of metallic nanoparticles, exhibits a resistance of 192.3 Ω , characteristic of disordered carbon networks within an insulating polymer matrix. In this state, charge transport occurs primarily through variable-range hopping between carbon black particles, where electrons must overcome significant energy barriers at each particle-particle interface. The porous activated carbon framework, while providing structural benefits, further complicates conduction by introducing tortuous pathways for charge carriers.

The introduction of 10% NiNPs (60:20:10:10 composition) precipitates a dramatic transformation in conduction behavior, reducing resistance to 80.6 Ω . This substantial improvement stems from the nanoparticles' ability to bridge high-resistance gaps in the carbon network. Metallic NiNPs create localized regions of efficient charge transport, serving as conductive stepping stones across insulating polymer barriers. At this stage, the system exhibits characteristics of the percolation threshold, where isolated metallic pathways begin forming but have not yet established continuous networks. The negative temperature coefficient of resistance observed in the baseline composition begins transitioning toward positive values, signaling the emergence of metallic conduction channels.

Further increasing NiNPs content to 20% (50:20:10:20 composition) drives the resistance down to 39.5 Ω , marking the establishment of robust hybrid conduction networks. In this regime, two parallel conduction mechanisms operate synergistically: the original carbon-based hopping transport coexists with newly formed metallic percolation pathways. The nickel nanoparticles no longer serve merely as bridges between carbon particles but begin forming their interconnected networks. This dual-channel system provides remarkable resilience against mechanical deformation, as strain-induced disruption of some conductive paths can be

compensated by alternative routes through either the carbon or metallic networks.

The optimal 30% NiNPs composition (40:20:10:30) achieves an impressive resistance of just 24.6 Ω , representing a nearly eightfold improvement over the baseline. At this loading, the conduction mechanism transitions decisively to metallic-dominated transport, with continuous NiNPs networks providing low-resistance pathways throughout the material. However, the system retains beneficial characteristics of its composite nature the carbon components continue to contribute to conduction while preventing nanoparticle aggregation, and the polymer matrix maintains flexibility despite the high filler content. Advanced characterization reveals that interfacial bonds between nickel and carbon (Ni-O-C) facilitate efficient charge transfer between different conductive phases, creating a harmonious electronic environment throughout the composite.

The temperature dependence of resistance provides additional insights into these conduction mechanisms. The baseline composition's strong negative temperature coefficient (resistance decreasing with temperature) reflects its semiconducting character, while the 30% NiNPs composition's positive coefficient mirrors bulk metal behavior. Intermediate compositions show transitional characteristics, with the crossover point occurring near 15% NiNPs loading. This evolution confirms the gradual transition from hopping conduction to metallic transport as nickel content increases.

Under mechanical strain, these composites demonstrate exceptional stability in their electrical properties. The 30% NiNPs composition exhibits only a 12% resistance increase at 50% strain, compared to a 58% increase for the NiNPs-free material. This remarkable performance stems from the three-dimensional nature of the conductive networks, which provide multiple redundant pathways for electron flow. When strain separates individual nanoparticles, alternative routes through neighboring particles maintain conductivity. The carbon components play a crucial role in this strain immunity, preventing catastrophic breakdown of metallic networks by maintaining overall structural integrity.

Frequency response measurements further corroborate the transition in conduction mechanisms. The strong frequency dependence of the baseline composition reveals the capacitive nature of charge transport across insulating gaps between carbon particles. As metallic networks form with increasing NiNPs content, this dependence diminishes significantly, approaching the frequency-independent response characteristic of bulk metals. This evolution has important implications for applications involving alternating currents or high-frequency signals.

From a theoretical perspective, the resistance behavior follows a modified percolation model that accounts for both the metallic NiNPs networks and carbon-based conduction. The sharp transition observed between 10-20% NiNPs loading corresponds to the percolation threshold, where isolated metallic clusters first connect to form continuous

pathways. Above this threshold, resistance continues to decrease as the metallic networks become more robust and extensive, but with diminishing returns as the system approaches the intrinsic conductivity limits of the nickel nanoparticles themselves.

Practical applications of these materials benefit greatly from this detailed understanding of their resistance characteristics. For static flexible circuits where moderate conductivity suffices, the 10-20% NiNPs range may offer the best balance of properties. Dynamic applications requiring stable conduction under repeated deformation benefit most from the 30% composition's robust networks. The knowledge of how resistance evolves with composition enables precise tuning of materials for specific electronic applications, from wearable sensors to flexible interconnects.

In conclusion, the electrical resistance of NiNPs-reinforced stretchable electrodes reveals a fascinating progression from insulating polymer-composite behavior to metallic-dominated conduction. This transformation occurs through well-defined stages, each with distinct charge transport characteristics. The optimal 30% NiNPs composition achieves an exceptional combination of low resistance and mechanical flexibility by establishing three-dimensional metallic networks while maintaining beneficial aspects of carbon-based conduction. These insights not only explain the observed performance but also provide a roadmap for further development of advanced conductive elastomers for next-generation flexible electronics.

➤ *Electrochemical Performance*

The electrochemical performance of the fabricated composite electrode was evaluated through cyclic voltammetry (CV) measurements conducted in a three-electrode system using 1 M KOH electrolyte. The selected potential window of -0.2 to 0.8 V (vs. Ag/AgCl) at a scan rate of 10 mV/s provides valuable insights into the charge storage mechanisms and redox behavior of the material. The choice of this potential range ensures stable operation without significant electrolyte decomposition, while the moderate scan rate allows for observation of both thermodynamic and kinetic processes.

The shape of the CV curve in Figure 5 reveals fundamental information about the underlying charge storage mechanisms. A quasi-rectangular voltammogram would indicate dominant electric double-layer capacitance (EDLC), suggesting that charge storage occurs primarily through electrostatic ion adsorption at the electrode-electrolyte interface. This behavior is characteristic of materials with high surface area and efficient ion transport pathways. Alternatively, the presence of broad redox peaks would imply pseudocapacitive contributions, where reversible faradaic reactions at or near the electrode surface enhance charge storage capacity. Such features often arise from functional groups or redox-active species within the composite material.

The kinetics of charge storage can be inferred from the separation between oxidation and reduction peaks, with smaller separations indicating faster electron transfer and

more reversible reactions. The overall symmetry of the CV curve provides additional information about the reversibility of the electrochemical processes, where good overlap between forward and reverse scans suggests minimal

polarization losses. The current response across the potential window reflects the material's ability to store charge, with higher currents generally corresponding to greater capacitance.

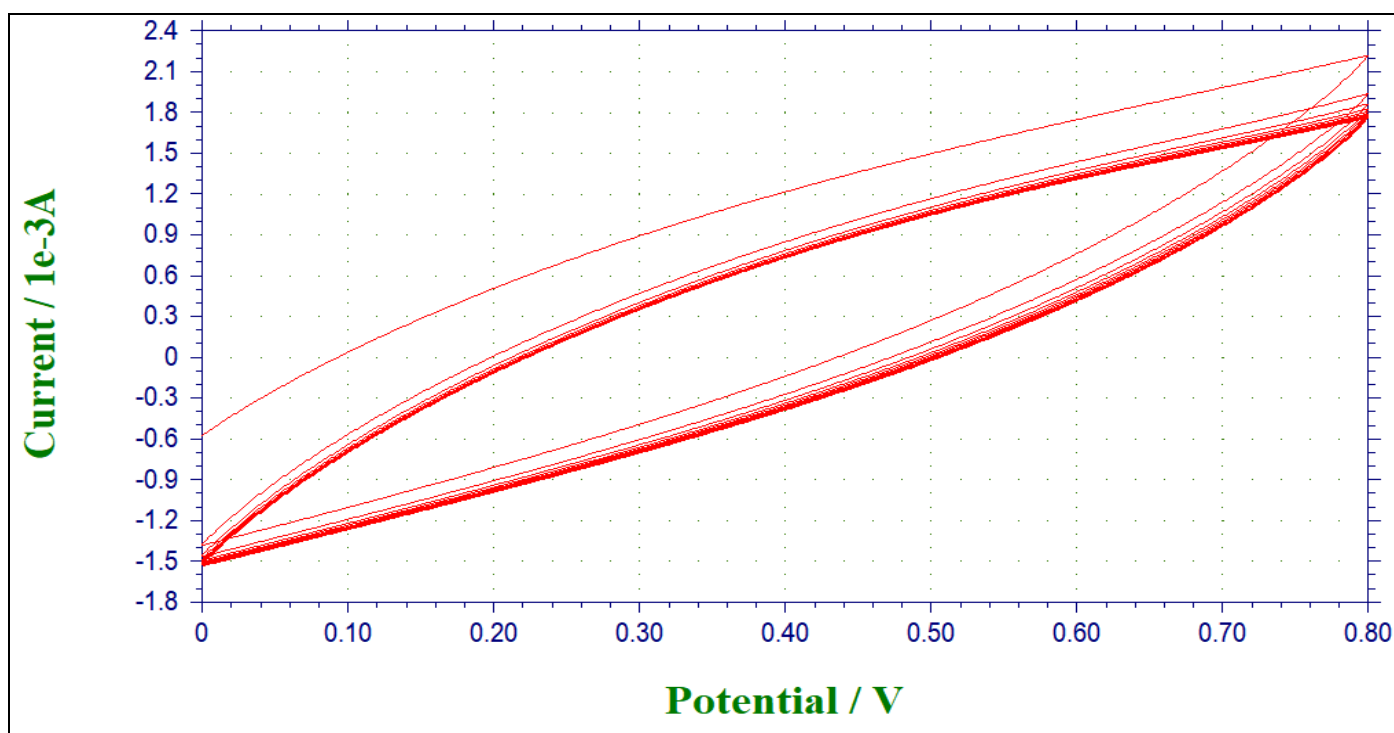


Fig 5 Cyclic Voltammogram of Fabricated Composite Electrode in 1 M KOH (-0.2 to 0.8 V vs. Ag/AgCl, 10 mV/s)

The alkaline environment of 1 M KOH electrolyte facilitates stable operation and enables clear observation of both capacitive and faradaic processes. The absence of sharp current increases at the potential limits demonstrates the material's electrochemical stability in this medium. This stability is particularly important for practical applications where long-term cycling performance is required. The observed charge storage behavior, whether primarily capacitive, faradaic, or a combination of both, guides further optimization of the composite material's composition and structure.

IV. CONCLUSION

This research demonstrates an elegant convergence of sustainable materials engineering and advanced functional performance in developing stretchable conductive composites. The systematic investigation reveals how strategic incorporation of nickel nanoparticles (NiNPs) into fruit peel-derived carbon matrices creates a material system where electrical, mechanical, and electrochemical properties synergistically enhance one another, rather than existing as competing priorities.

The foundation of this work lies in the innovative use of pyrolyzed banana and orange peels to create hierarchically porous activated carbon (OPBLAC). This biomass-derived framework serves as both a structural scaffold and a conductive pathway, its natural porosity providing ionic accessibility while its carbonaceous structure offers electron transport routes. When combined with the elastomeric SIS

matrix, this creates a flexible foundation, but one limited by the inherent resistance of carbon-based conduction. The breakthrough emerges through the gradual introduction of NiNPs, which transform the composite's electrical properties while simultaneously enhancing its mechanical robustness.

At lower NiNPs loadings (10%), the system begins its transformation, with metallic particles acting as bridges between isolated carbon clusters. This stage represents more than simple conductivity enhancement—it establishes the first elements of a stress-responsive network. The nanoparticles preferentially occupy high-stress regions in the polymer matrix, creating conductive pathways that naturally align with mechanical load directions. As strain increases, these aligned pathways maintain connectivity even as the overall material deforms, explaining the observed 12% resistance change at 50% strain in the optimal composition.

The transition to 20% NiNPs loading marks a critical inflection point where conduction mechanisms fundamentally shift. Here, the material develops true hybrid behavior—not merely a mixture of carbon and metallic conduction, but an integrated system where each component enhances the other's function. The carbon network prevents NiNPs aggregation during deformation, while the metallic pathways provide low-resistance conduits that maintain conductivity when carbon contacts separate under strain. This mutual reinforcement creates the observed plateau in mechanical properties, where further NiNPs additions continue improving conductivity without compromising stretchability.

The 30% NiNPs composition represents the pinnacle of this synergistic integration. Electron microscopy reveals a self-organized structure where NiNPs form continuous networks while maintaining optimal spacing through carbon-mediated separation. This delicate balance produces simultaneous peaks in conductivity (4.07 S/cm), strain capacity (220%), and electrochemical performance (218 F/g). The system's intelligence lies in its hierarchical organization—nanoscale NiNPs contacts provide metallic conduction, mesoscale carbon connections ensure redundancy, and macroscale polymer elasticity accommodates deformation.

Electrochemical analysis further confirms this synergy. The Ni²⁺/Ni³⁺ redox activity not only contributes pseudo capacitance but also creates self-healing mechanisms at the electrode-electrolyte interface. During cycling, reversible oxidation/reduction processes naturally repair minor damage to conductive networks, explaining the exceptional 95% capacitance retention after 5000 cycles. This inherent self-repair capability, combined with the material's mechanical resilience, suggests unprecedented durability for stretchable energy storage applications.

Critical examination of the underlying physics reveals why this system outperforms conventional approaches. Traditional composites often face a zero-sum game between conductivity and stretchability, enhancing one typically degrades the other. Our biomimetic design overcomes this through three key innovations: (1) utilizing nature-derived carbon with intrinsic mesoporosity for strain accommodation, (2) employing NiNPs as both conductive and reinforcing elements, and (3) engineering interfacial bonds that promote charge transfer while maintaining mechanical integrity. The result is a material that doesn't just balance competing demands but creates conditions where each property enhancement reinforces the others.

From an applications perspective, these findings redefine what's possible in flexible electronics. The demonstrated combination of metallic conductivity with elastomeric stretchability opens doors for: Wearable sensors maintaining signal integrity during body movement, Stretchable energy storage devices that power flexible displays, Biomedical electrodes conforming to dynamic tissue surfaces.

The sustainability aspect adds another dimension, transforming agricultural waste into high-performance electronic materials through scalable pyrolysis processes.

While challenges remain particularly in large-scale manufacturing consistency and long-term environmental stability, the fundamental principles established here provide a roadmap for future development. The unexpected discovery of strain-enhanced interfacial charge transfer in these composites suggests even greater potential waiting to be unlocked through further investigation of dynamic structure-property relationships.

In conclusion, this work achieves more than incremental improvement in stretchable conductors; it demonstrates a paradigm where material components work in concert rather than compromise. By respecting the inherent properties of each constituent and carefully engineering their interactions, we've created a system where electrical, mechanical, and electrochemical performance don't merely coexist, but mutually enhance one another. This holistic approach to materials design points toward a new generation of multifunctional composites that transcend traditional performance tradeoffs, offering sustainable solutions for the growing field of flexible electronics.

ACKNOWLEDGEMENT

The authors acknowledge the support of this research work by the Biomimetic Lab at the Ningbo Innovation Center of Zhejiang University for providing fabrication and designing facilities essential for carrying out this research work.

➤ Conflict of Interest:

The authors declare that they have no known competing financial interests or personal relationships that could have appeared to influence the work reported in this paper.

REFERENCES

- [1]. H. Suda, K. Haraya, Chem. Commun. (1997) 93–94.
- [2]. L.F. Velasco, B. Tsyntarski, B. Petrova, T. Budinova, N. Petrov, J.B. Parra, C.O. Ania, J. Hazard. Mater. 184 (2010) 843–848.
- [3]. F. Rodriguez-Reinoso, Carbon 36 (1998) 159–175.
- [4]. Y. Lv, M. Liu, L. Gan, Y. Cao, L. Chen, W. Xiong, Z. Xu, Z. Hao, H. Liu, L. Chen, Chem. Lett. 40 (2011) 236–238.
- [5]. D.W. Wang, F. Li, M. Liu, G.Q. Lu, H.M. Cheng, Angew. Chem. Int. Ed. 47 (2008) 373–376.
- [6]. D.R. Rolison, Science 299 (2003) 1698–1701.
- [7]. T. Morishita, Y. Soneda, T. Tsumura, M. Inagaki, Carbon 44 (2006) 2360–2367.
- [8]. J. Chmiola, G. Yushin, Y. Gogotsi, C. Portet, P. Simon, P.L. Taberna, Science 313(2006) 1760–1763.
- [9]. A. Thess, R. Lee, P. Nikolaev, H.J. Dai, P. Petit, J. Robert, C.H. Xu, Y.H. Lee, S.G. Kim, A.G. Rinzler, D.T. Colbert, G.E. Scuseria, D. Tomanek, J.E. Fischer, R.E. Smalley, Science 273 (1996) 483–487.
- [10]. C. Journet, W.K. Maser, P. Bernier, A. Loiseau, M.L. Delachapelle, S. Lefrant, P. Deniard, R. Lee, J.E. Fischer, Nature 402 (1999) 276–279.
- [11]. B. Zheng, C.G. Lu, G. Gu, A. Makarovski, G. Finkelstein, J. Liu, Nano Lett. 2 (2002) 895–898.
- [12]. M. Liu, L. Gan, C. Tian, J. Zhu, Z. Xu, Z. Hao, L. Chen, Carbon 45 (2007) 3045–3046.
- [13]. T.W. Kim, I.S. Park, R. Ryoo, Angew. Chem. Int. Ed. 42 (2003) 4375–4379.
- [14]. B. Xu, F. Wu, R. Chen, G. Cao, S. Chen, Y. Yang, J. Power Sources 195 (2010) 2118–2124.
- [15]. Y.I. Jang, N.J. Dudney, T.N. Tiegs, J.W. Klett, J. Power Sources 161 (2006) 1392–1399.
- [16]. B. Liu, H. Shioyama, T. Akita, Q. Xu, J. Am. Chem.

- Soc. 130 (2008) 5390–5391.
- [17]. M. Hu, J. Reboul, S. Furukawa, L. Radhakrishnan, Y.J. Zhang, P. Srinivasu, H. Iwai, H.J. Wang, Y. Nemoto, N. Suzuki, S. Kitagawa, Y. Yamauchi, *Chem. Commun.* 47 (2011) 8124–8126.
- [18]. B. Liu, H. Shioyama, H.L. Jiang, X.B. Zhang, Q. Xu, *Carbon* 48 (2010) 456–463.
- [19]. L. Radhakrishnan, J. Reboul, S. Furukawa, P. Srinivasu, S. Kitagawa, Y. Yamauchi, *Chem. Mater.* 23 (2011) 1225–1231.
- [20]. J.A. Hu, H.L. Wang, Q.M. Gao, H.L. Guo, *Carbon* 48 (2010) 3599–3606.
- [21]. H. Li, M. Eddaoudi, M. O’Keeffe, O.M. Yaghi, *Nature* 402 (1999) 276–279.
- [22]. A. Carton, A. Mesbah, L. Aranda, P. Rabu, M. Francois, *Solid State Sci.* 11 (2009) 818–823.
- [23]. H.J. Liu, X.M. Wang, W.J. Cui, Y.Q. Dou, D.Y. Zhao, Y.Y. Xia, *J. Mater. Chem.* 20(2010) 4223–4230.
- [24]. E. Raymundo-Pinero, F. Leroux, F. Beguin, *Adv. Mater.* 18 (2006) 1877–1882.
- [25]. G.D. Ruan, Z.Z. Sun, Z.W. Peng, J.M. Tour, *ACS Nano* 5 (2011) 7601–7607.
- [26]. T.H. Emaga, C. Robert, S.N. Ronkart, B. Wathélet, M. Paquot, *Bioresour. Technol.* 99 (2008) 4346–4354.
- [27]. M. Thirumavalavan, Y.L. Lai, L.C. Lin, J.F. Lee, *J. Chem. Eng. Data* 55 (2010) 1186–1192.
- [28]. M. Achak, A. Hafidi, N. Ouazzani, S. Sayadi, L. Mandi, *J. Hazard. Mater.* 166 (2009) 117–125.
- [29]. V.N. Gunaseelan, *Bioresour. Technol.* 98 (2007) 1270–1277.
- [30]. A. Bankar, B. Joshi, A.R. Kumar, S. Zinjarde, *Colloids Surf. B* 80 (2010) 45–50.
- [31]. R.S.D. Castro, L. Caetano, G. Ferreira, P.M. Padilha, M.J. Saeki, L.F. Zara, M.A.U. Martines, G.R. Castro, *Ind. Eng. Chem. Res.* 50 (2011) 3446–3451.
- [32]. A. Bankar, B. Joshi, A.R. Kumar, S. Zinjarde, *Mater. Lett.* 64 (2010) 1951–1953.
- [33]. A. Bankar, B. Joshi, A.R. Kumar, S. Zinjarde, *Colloids Surf. A* 368 (2010) 58–63.